Macromolecular Rapid Communications
www.mrc-journal.de

Correlating Molar Mass, π-Conjugation, and Optical Properties of Narrowly Distributed Anionic Polythiophenes in Aqueous Solutions

Martina Schmidt, Matthias Karg, Mukundan Thelakkat, and Johannes C. Brendel**

Polythiophene-based conjugated polyelectrolytes (CPE) are attracting increasing attention as sensor or interface materials in chemistry and biology. While cationic polythiophenes are better understood, limited structural information is available on their anionic counterparts. Limited access to well-defined polymers has made the study of structure-property relationships difficult and clear correlations have remained elusive. By combining controlled Kumada catalyst transfer polymerization with a polymer-analog substitution, regioregular and narrowly distributed poly(6-(thiophen-3-yl)hexane-1-sulfonate)s (PTHS) with tailored chain length are prepared. Analysis of their aqueous solution structures by small-angle neutron scattering (SANS) revealed a cylindrical conformation for all polymers tested, with a length close to the contour length of the polymer chains, while the estimated radii remain too small (<1.5 nm) for extensive π-stacking of the chains. The latter is particularly interesting as the longest polymer exhibits a concentration-independent structured absorption typical of crystalline polythiophenes. Increasing the ionic strength of the solution diminishes these features as the Coulomb repulsion between the charged repeat units is shielded, allowing the polymer to adopt a more coiled conformation. The extended π-conjugation, therefore, appears to be a key parameter for these unique optical features, which are not present in the corresponding cationic polythiophenes.

1. Introduction

Conjugated polyelectrolytes (CPEs) are an interesting class of materials, which combine the high charge density of polyelectrolytes with an extended π-system in the backbone. These materials find applications in photovoltaic devices, organic light-emitting diodes, photodetectors, actuators, or electrochromic devices.[1–6] Furthermore, their excellent water compatibility renders them particularly attractive as (bio)sensor materials.[7–13] Numerous CPEs have already been developed and investigated in detail beginning with the early work on conjugated ionic poly(*p*-phenylene) (PPP) or poly(*p*-phenylene ethynylene) (PPE) derivatives,[14–23] and continued with polyfluorenes (PF) and polythiophenes (PT).[24–26] The latter have already been prepared in 1987 using electropolymerization of ionic monomers,[27] while in the last decades, they have moved into the focus of research on sensor materials.[28] Polythiophenes are particularly attractive as the tilted conformation of the repeating unit allows for alterations of the backbone conformation, which induce a significant change in the conjugation

M. Schmidt, M. Thelakkat
Applied Functional Polymers (AFUPO)
University of Bayreuth
95440 Bayreuth, Germany
E-mail: mukundan.thelakkat@uni-bayreuth.de
M. Karg
Physical Chemistry I
Heinrich-Heine-University Düsseldorf
Universitätsstr. 1, 40225 Düsseldorf, Germany
J. C. Brendel
Laboratory of Organic and Macromolecular Chemistry (IOMC)
Friedrich Schiller University Jena
Humboldtstraße 10, 07743 Jena, Germany
E-mail: johannes.brendel@uni-jena.de
J. C. Brendel
Jena Center for Soft Matter (JCSM)
Friedrich Schiller University Jena
Philosophenweg 7, 07743 Jena, Germany

The ORCID identification number(s) for the author(s) of this article can be found under https://doi.org/10.1002/marc.202300396

DOI: 10.1002/marc.202300396

and thus in their optical properties.[29] So far, most reports are related to the application of cationic polythiophenes as sensor materials for detecting proteins or genetic material, in which the polymer undergoes a conformation change with addition and complexation of the analyte. This induces, for example, a shift of the absorption or a change in the fluorescence signal.[28,30–32] For such applications, anionic polythiophenes are rarely reported, although they gain increasing interest as complementary materials to the more established cationic polymers. Among them, carboxylate modified polythiophenes were for example tested for ionchromatic sensing,[33–35] discriminating protein conformational states,[36–38] or, more recently, for an assay to test bacteria´s protease activity, although the polymers require alkaline conditions to be soluble.[39] Alternative malonate modifications improve the solubility of these polythiophene derivatives, which enables more versatile applications, as for example the sensing of carbon dioxide.[40,41] Interesting anionic polythiophenes based on thiosulfate groups (Bunte-type salts) have also been reported,[42] which insert into biological lipid bilayers and allow sensing of phase transitions.[43,44]

Overall, the majority of CPEs based on polythiophene are prepared by oxidative polymerization, which tolerates many ionic groups, but leads to broadly dispersed polymers with a regioregular conformation of the repeating units. This lack of control on the polymer structure and length, however, limits the ability to draw direct correlations between optical properties and the structure or conformation of the polymer chains in solution. The importance of a regioregular conformation is exemplified in the studies of Knaapila et al., which compare solution structures of a regioregular, cationic polythiophene derivatives and the respective optical properties in presence of different surfactant concentrations.[45–47] Similarly, McCullough et al. reported on the importance of a regioregular nature of an anionic polythiophene derivative for the ionchromatic effect.[34,48] Generally, a precise control of the polymer structure is considered key for developing a better fundamental understanding of structure-property relations and designing next-generation CPEs for sensing applications.

Using a postpolymerization modification, we have demonstrated that regioregular anionic polythiophenes called poly(6-(thiophen-3-yl)hexane-1-sulfonates) (PTHS) can be prepared by Kumada Catalyst Transfer Polymerization (KCTP) leading not only to a highly regioregular structure but further allows for a tuning of molar mass, while maintaining narrow molar mass distributions.[49] In this case, the sulfonate groups are introduced by a postpolymerization nucleophilic substitution on poly(3-(6-bromohexyl)thiophene)s. Beside an excellent solubility in aqueous solutions, interesting optical features were observed, such as strong dependence of the absorption spectra on the molar mass of the polymers, but the focus of our previous studies was on the solid-state properties and conductivity of these CPEs.[50–52] Prompted by the recent developments in solution applications of similar CPEs and the related quest for more defined polymers,[28] we now had a closer look at the solution structure of these polymers, as they can easily be prepared with various length, while maintaining a narrow distribution. We considered that this access to quite defined CPEs of different lengths opens an interesting door to develop a better understanding of correlations between solution structures and corresponding optical features.

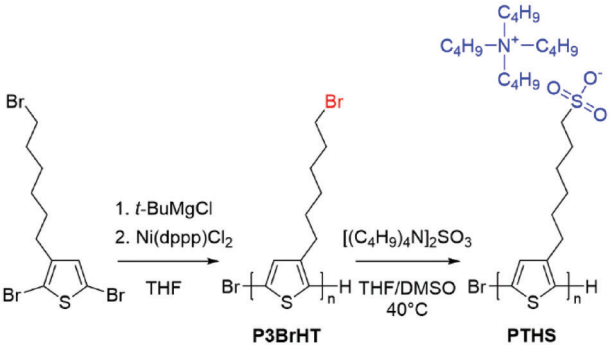

Scheme 1. Synthesis of well-defined PTHS.

Therefore, three different polymers with molar masses ranging from 6.3 to 41 kg mol^{-1} were analyzed. The structure in solution was characterized by small-angle neutron scattering (SANS). The photophysical properties of these PTHS in solution were examined in detail including concentration dependent absorption measurements. We focused in this study on the tetrabutylammonium counterions to guarantee a high solubility of all CPEs in an aqueous solution.[52] Furthermore, the impact of an increasing ionic strength was analyzed, which helps to evaluate the impact of the ionic repulsion on the polymer conformation, and finally a potential complex formation with a complementary cationic polythiophene was investigated.

2. Results and Discussion

The controlled chain growth mechanism of KCTP enables the preparation of conjugated polythiophenes, particularly poly(3-alkylthiophenes), with definite molar masses, narrow dispersity and defined end-groups.[53,54] Three poly(3-(6-bromohexyl) thiophene)s (P3BrHT) with different degrees of polymerization were prepared using this method and converted to the conjugated polyelectrolyte PTHS as reported previously.[49] Size exclusion chromatography (SEC) and matrix assisted laser desorption ionization with time-of-flight detection mass spectroscopy (MALDI-Tof-MS) measurements on the precursors (P3BrHT) are included in the supporting information (Figures S1 and S2 and Table S1, Supporting Information) confirming a narrow dispersity and providing information on the overall molar mass. The number of repeating units were also determined from MALDI-Tof-MS analysis. An overview of the synthetic procedure is presented in **Scheme 1** and characteristics of the final polyelectrolytes are summarized in **Table 1**.

We have already reported on the optical properties of these polymers in various solvents, but focus here on their behavior in aqueous solutions.[49] This is particularly intriguing as a strong shift in absorption was observed with increasing molar mass, which is also reflected in the gradual color change from yellow in case of PTHS 1 to deep purple for PTHS 3 (Photographs in **Figure 1**). The latter also reveals a structured absorption with a maximum at 552 nm as well as a pronounced shoulder at around 580 nm, which typically arises for aggregated polythiophene chains.[55–57] Such a clearly structured absorption as observed for PTHS 3 has so far only been reported for highly charged sulfonated polythiophenes.[58] While for carboxy-

Table 1. Summary of the determined characteristics of the final polymers PTHS 1–3.

CPE	n [a]	M_n [b] [kg mol^{-1}]	Đ [c]	Contour length [d] [nm]
PTHS 1	13	6.3	1.27	4.6
PTHS 2	30	15	1.07	10.7
PTHS 3	84	41	1.09	29.9

[a] Average number of repeating units calculated from the M_n of the precursors P3BrHT obtained in MALDI-ToF-MS analysis (see Table S1, Supporting Information); [b] Calculated from n and the molar mass of the repeating unit of PTHS; [c] Dispersity was taken from SEC analysis of the corresponding precursors P3BrHT; [d] Calculated from n and average size of a single repeating unit of 0.356 nm.

lated polythiophenes these signals are weaker, cationic polythiophene derivatives show no sign of aggregation unless complexing agents such as sodium dodecyl sulfate are added.[45,59] To further analyze this behavior, we measured the absorption at different concentrations. The shortest CPE PTHS 1 (Figure 1a; see Figure S3a, Supporting Information for absolute absorptions) displayed similar common solutions spectra for polythiophenes at all tested concentrations (1-2500 mg L^{-1}), which indicates that even at high concentrations no significant aggregation occurs. PTHS 2 with 30 repeating units (Figure 1b; see Figure S3b, Supporting Information for absolute absorptions), on the contrary, displayed a more significant change with increasing polymer concentration. Starting at 1 mg L^{-1}, a shoulder at around 530 nm is already visible, which becomes enhanced at higher concentrations. This shoulder indicates π–π interactions, which in the case of this medium sized CPE, however, appears to depend on the polymer concentration. Therefore, we assume intermolecular interactions cause the observed red shift for these polymers. Interestingly, no influence of concentration becomes apparent in case of the largest CPE PTHS 3 (n = 84), despite concentration differences of several orders of magnitude (0.0001–0.25 w/v%). The maximum remains at 552 nm and the shoulder at around 580 nm is similarly pronounced for all tested concentrations (Figure 1c; see Figure S3c, Supporting Information for absolute absorptions). For P3HT, it has been shown that chain folding starts at an M_n (SEC) of ≈20 kg mol^{-1}.[60] In analogy to this, chain folding might be a reasonable factor for the concentration independent aggregation of PTHS 3.

The significant differences in their optical appearance prompted us to analyze the solution structure of the polymers with different molar masses. In particular, the concentration-independent formation of aggregates in case of PTHS 3 is intriguing and may help to gain a better understanding of structure-property relationships in CPEs. Initial attempts to resolve any potential aggregates by transmission electron microscopy (TEM) did not reveal any particulate structure or larger aggregates (Figure S4, Supporting Information). Consequently, we followed previous attempts to analyze solution states of CPEs and applied SANS for structural investigations covering different length scales (**Figure 2**). Therefore, all three polymers (PTHS 1-3) were dissolved in D_2O at a concentration of 3 g L^{-1}. In addition, we also investigated a solution of PTHS 3 in deuterated DMSO (Figure S5, Supporting Information), since this polymer showed the most significant change in the optical properties when comparing both solutions.

All measurements reveal a similar upturn of the scattering intensity in the higher q-range at around 2 nm^{-1}, which scales with q^{-3}. Such a step increase indicates the presence of distinct structures, and any attempts to fit the data with a Gaussian coil model therefore failed in this part. While the formation of such structures was expected for PTHS 3, we were surprised that this feature is also present in the samples PTHS 1 and PTHS 2, where the optical properties did not indicate any sign of aggregation. In the intermediate q-range (0.1–1 nm^{-1}), however, the scattering data becomes more differentiated. Although all samples are characterized by a maximum, its position shifts toward lower q-values with increasing molar mass. Similar maxima have previously been observed in SANS studies on cationic polythiophenes and can be attributed to electrostatic repulsion and an excluded volume effect.[45,46] A corresponding structure factor (Hayter-Penfold Rescaled Mean Spherical Approximation) was tested to match the observed peak maxima.[62] The resulting charge values are increasing with the size of the polymers, which seems plausible given the increasing number of repeating units or ionic groups. All measurements are further characterized by a power-law like upturn at low q values, which scales with q^{-3} and most likely points at some remaining fractal aggregates in the solution. Similar observations were again made for the above-mentioned cationic polythiophenes.[45,46]

We tried to fit the data with a cylinder model, which was combined with the above-mentioned Hayter-Penfold structure factor for macroions and an additional power-law scaling (q^{-3}) to match the upturn at low q values (overview of fit parameters is given in Tables S2–S8, individual contributions to the fits are separately

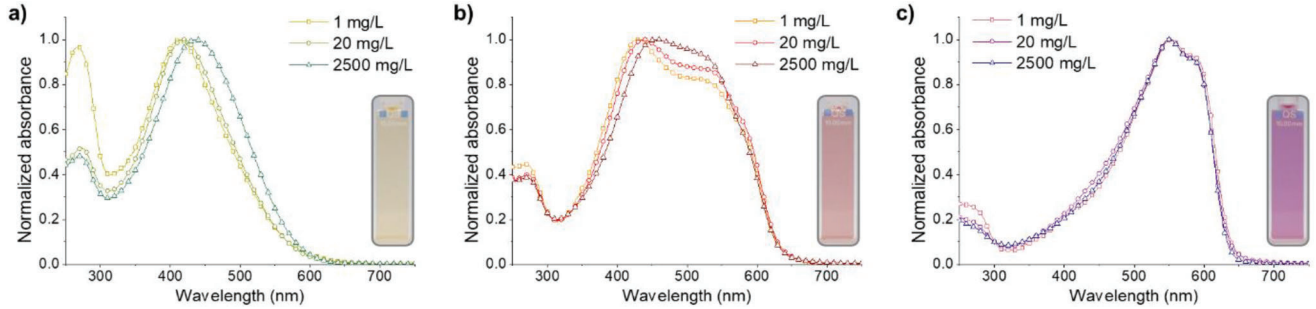

Figure 1. Normalized (divided by maximum) absorbance spectra of various concentrations of a) PTHS 1 (n = 13), b) PTHS 2 (n = 30), and c) PTHS 3 (n = 84) in aqueous solution: 1 mg L^{-1} (squares), 20 mg L^{-1} (circles), and 2500 mg L^{-1} (triangles). The insets show photographs of solutions at 20 mg L^{-1}. The corresponding absolute absorption spectra are given in Figure S3 (Supporting Information).

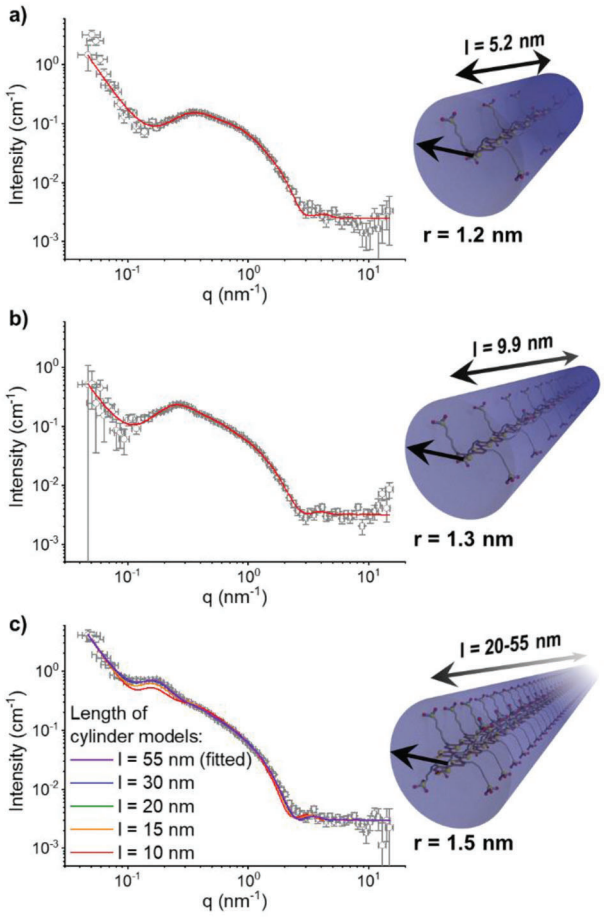

Figure 2. SANS profiles of solutions of a) PTHS 1 (n = 13, c = 3 g L^{-1}), b) PTHS 2 (n = 30, c = 3 g L^{-1}), and c) PTHS 3 (n = 84, c = 3 g L^{-1}) in D_2O. The continuous lines represent fits for each sample combining a cylindrical model with a Hayter-Penfold structure factor and an additional power-law scaling (q^{-3}), which were calculated with SASfit (detailed parameters are given in Tables S2–S8, Supporting Information).[61] In case of c) PTHS 3 multiple fits with set length were added (An individual representation is given in Figure S7, Supporting Information).

plotted in Figures S6 and S7, Supporting Information).[62] All scattering curves could be fitted nicely with this combination. The fitted radii were in a similar range of 1.2–1.5 nm for all samples, while the length varies significantly with the degree of polymerization. A length of 5.2 nm is estimated from the fit for the shortest polymer PTHS 1 (Figure 2a; Table S2, Supporting Information). This value is in good agreement with a fully stretched chain (4.6 nm for n = 13). The difference might be related to an underestimation of the average degree of polymerization or deviations in the fit due to the background. A similar close match is found for PTHS 2 with a fitted length of 9.9 nm compared to 10.7 nm for a fully stretched chain (Figure 2b; Table S3, Supporting Information). Both PTHS 1 and 2 resulted in rather small, fitted radii of 1.2 or 1.3 nm, respectively, which should reflect a single chain without any aggregation considering a stretched hexyl side chain (≈1 nm) plus the bulky tetrabutylammonium counterion. This agrees well with their optical properties, although in case of PTHS 2 the presence of stacks of two chains cannot be fully excluded. More interesting is the sample PTHS 3, which already indicated the presence of π-stacking in its absorption spectrum. To our surprise, the radius of the structures determined in SANS is only slightly larger (1.5 nm) than for the other two samples (Figure 2c). Notwithstanding a considerable error width in the data in this high q-range, the number of stacked chains appears to be limited. We assume that only around two to three conjugated chains fit into the estimated radius considering again the size of stretched hexyl side chains (≈1 nm) plus the bulky tetrabutylammonium counterions. The result further explains the absence of any structures in the TEM images, as visualization of soft materials with such small feature sizes is extremely challenging and could not be realized with the given instrumentation. Nevertheless, a stacking of chains is still very likely and might be a result of intermolecular interactions or intramolecular chain folding. The length of the structures should shed light on this aspect, but the overlap of the peak maxima with the rollover of the cylinder length limits the accuracy of the fits and results in a broad error of the fitted length. Fitting the length resulted in a value of 54.6 ± 8.0 nm, which is significantly larger than the stretched chain itself (29.9 nm). Such a discrepancy cannot be explained by a potential underestimation of the degree of polymerization. The extended length of the structures might also be a result of an offset in the stacking of chains, but a near doubling of the maximum chain length seems still unlikely, if only two or very few chains stack on top of each other. Therefore, we also tested a cylinder model with a fixed length of 30 nm corresponding to the stretched chain. As visible in Figure 2c (see also Figure S7, Supporting Information for individual representation of the fits), there is no significant difference compared to the initial fit and similar R-values (0.091 compared to 0.088) were obtained. In consequence, we systematically examined fits with shorter set length. Setting the value to 20 nm did not yet change the quality of the fit significantly if other parameters were adapted slightly (see Tables S4–S8, Supporting Information for details). This result indicates that chain folding might be possible within the given structures. However, reducing the length further to 15 or 10 nm did result in visible deviations of the fit from the scattering data, which could not be compensated by adjusting other parameters. For comparison, we also analyzed PTHS 3 in DMSO (Figure S5, Supporting Information). The SANS data in this solvent reflected more the expectations for a coil like conformation (see Table S9, Supporting Information for details of the fit), although again a structure factor is required for a proper fit of the data.

Overall, these results suggest that PTHS adopts a rather rigid cylindrical structure in an aqueous solution due to the electrostatic repulsion, which comprises only a single chain or few aggregated chains in a stretched conformation. The polymers should therefore be conjugated over nearly their entire length with limited disturbance. Structural similarities are given to cationic polythiophenes in aqueous solutions with addition of the anionic surfactant sodium dodecylsulfate.[45,46] Rod-like structures with comparable radii were found in presence of small amounts of the surfactant, which further caused similar vibronic structures in the corresponding absorption spectra of the solutions. It is noteworthy to mention that this structured absorption must arise from only a few π-stacked chains and does not require multiple layers as found in semi-crystalline bulk samples or films of other polythiophenes.

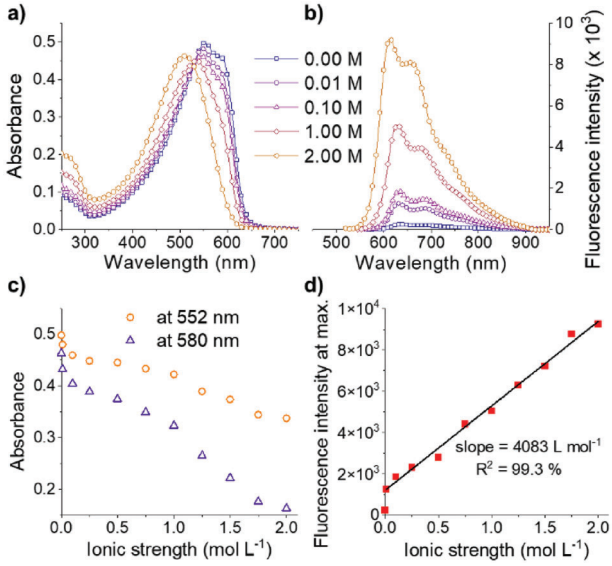

Figure 3. a) UV–vis and b) fluorescence spectra (excitation at maximum absorbance) of PTHS 3 (n = 84) in aqueous solutions (c = 20 mg L^{-1}) with increasing concentrations of tetrabutylammonium chloride ($N(Bu)_4Cl$): without salt (squares), 0.01 M (circles), 0.10 M (triangles), 1.00 M (diamonds), 2.00 M (hexagons). Correlation between the ionic strength of the solution and c) the absorbance at the maximum (552 nm) plus the shoulder (580 nm) or d) the maximum fluorescence intensity, which could be fitter with a linear regression (black line).

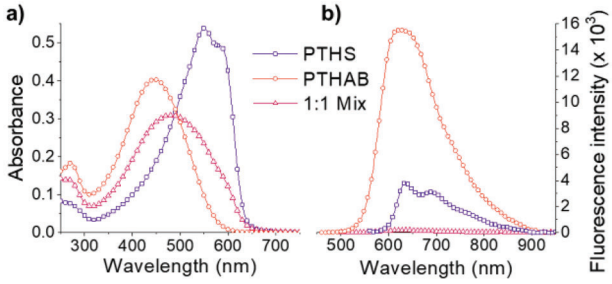

Figure 4. a) UV–vis and b) fluorescence spectra (excitation at maximum absorbance) of aqueous solutions of PTHAB (circles, n = 84, c = 20 mg L^{-1}) in comparison to PTHS 3 (squares, n = 84, c = 20 mg L^{-1}), as well as the spectra of a mixed solution (triangles) at equal amounts (1:1 molar ratio).

The high charge density seems further key to induce the stretched conformation and the resulting structure. This conformation of polymer chains in general strongly depends on the interaction with the surrounding medium. In the special case of polyelectrolytes, the hydration effects of water are known to increase the counter ion dissociation. In consequence, the charge density on the polymer chain is increased, which causes repulsive coulomb forces and the stretching of the polymer chain.[63,64] Ion dissociation and repulsive interactions, however, depend largely on the concentration of counterions and the ionic strength, which is directly reflected in the different chain conformations of non-conjugated polyelectrolytes in solutions of different ionic strength.[65] Increasing salt concentrations may therefore alter these parameters and, thus, limit the impact of the high charge density of common polyelectrolytes.[66] In general, conjugated polyelectrolytes possess stiffer polymer backbones in contrast to non-conjugated polymers. However, polythiophenes are still characterized by a coiled conformation in dilute solution due to the twisted bond angle between two repeating units.[29] Considering the above-mentioned facts the question arises whether the addition of salt has a similar effect on the polymer conformation of PTHS. Therefore, we dissolved PTHS 3 in aqueous solutions containing different amounts tetrabutylammonium chloride (0–2 M) and analyzed the optical properties (**Figure 3**; additional concentrations are given in Figure S8, Supporting Information). The tetrabutylammonium salt was chosen to avoid any additional effects due to counterion exchange.

In the absorption spectra (Figure 3a), a decrease of the signals at 552 nm (peak) and 580 nm (shoulder) and the appearance of a new signal at 510 nm with an isosbestic point at 529 nm are observed upon addition of the salt. Electrostatic repulsion between the charged repeating units is enhanced in salt-free aqueous solutions and favors a stretching of the polymer chains that abets the π-π interaction and aggregation causing the observed structured absorption. The salt-induced change in the absorption spectra must consequently relate to a change of the aggregation state and the backbone conformation, as with increasing ionic strength electrostatic repulsive forces are diminished. We assume that the new signal at 510 nm, therefore, corresponds to a non-aggregated species in this aqueous solution, which could not be observed earlier in the absence of salt. Correspondingly, the fluorescence signal of the solution increases steadily and shifts toward shorter wavelengths (Figure 3b). This increase further corroborates our assumption that aggregates, which are present in salt-free water, get disrupted and a more flexible chain conformation is adopted. Aggregation is known to quench the fluorescence and, consequently, the above-mentioned disintegration of these aggregates at increasing salt concentrations induces a steady increase of fluorescence intensity. A direct comparison of the absorbance maximum (552 nm) and the characteristic shoulder at 580 nm with the ionic strength of the solutions reveals a strong change at low salt concentrations, followed by a continuous decrease with further increase of the tetrabutylammonium chloride content (Figure 3c). A similar correlation is found for the maximum fluorescence intensity (Figure 3d), although in this case, the intensity increases linearly with ionic strength after the initial jump when small amounts of salt are added. This trend could well be fitted with a linear regression having a slope of 4083 L mol^{-1}. As mentioned above, the changes in the spectra are most likely due to disintegration of polymer aggregates in the presence of tetrabutylammonium chloride salt, but other ions, especially multivalent ions, may have different effects or even induce additional aggregation, limiting generalization of this trend.

In a final step, we also prepared a complementary cationic polythiophene starting from the precursor of PTHS 3 with a degree of polymerization of 84. In this case the bromine group was reacted with trimethyl amine to generate poly(*N*,*N*,*N*-trimethyl-6-(thiophen-3-yl)hexan-1-aminium bromide) (PTHAB) carrying a quarterly ammonium ion on the side chain. Similar to previously reported cationic polythiophenes,[45,46] the polymer featured a broad absorption maximum at 446 nm, but lacked the structured absorption found for PTHS 3b (**Figure 4**a). Further-

more, a more pronounced photoluminescence is observed for this polymer, when compared to PTHS 3 at similar concentrations (Figure 4b). The ionic nature has therefore a critical influence on the conformation in solution and the resulting optical properties. We further combined both solutions containing PTHS 3 and PTHAB, as the formation of coacervates between CPEs and oppositely charged polyelectrolytes has attracted increasing attention over the last years.[67,68] Against our expectations no precipitation or larger aggregates were formed, but the solution remained homogeneous and stable. Since both polymers are highly charged, strong interactions can be expected due to the gain of entropy by releasing the corresponding counterions, when bringing both complementary CPEs together. However, the identical backbone length and homogenous structure might prevent formation of larger phase-separated aggregates.[69] It is further interesting to note that the absorbance spectra of the mixed polymer solution did not reveal significant changes in the structure of the polymers when comparing it to the spectra of the individual polyelectrolyte solutions. It mostly represents a superposition of both absorption spectra, which does not hint at significant conformational changes. However, the photoluminescence in the solution is significantly quenched in contrast to both individual solutions. We therefore assume that the oppositely charged polymers must interact, but form highly hydrated complexes, which does not impair with their individually preferred conformations.

3. Conclusion

In summary, the access to the regioregular PTHS with narrow molar mass distribution revealed a distinct correlation between length of the polymer chains, their solution conformation, and their optical properties. The combination of the Kumada catalyst transfer polymerization and polymer analogs reactions to introduce the ionic group appeared in this regard to be an effective approach to generate these defined CPEs. The significance of distinct polymer length becomes already apparent, when analyzing the concentration-dependent absorbance of aqueous solutions. While short chains (PTHS 1, n = 13) did not show significant signs of aggregation even at high concentrations, the medium sized polymer (PTHS 2, n = 30) displayed a concentration-dependent aggregation behavior. Interestingly, the largest PTHS 3 (n = 84) formed similar aggregates at all tested concentrations (1–2500 mg L^{-1}). Investigation of the solution structure by SANS revealed stretched polymer conformations for the short (PTHS 1) and medium-sized (PTHS 2) polymers, as the length of the cylinder model in the fits and the calculated chain lengths match. In the case of the long PTHS 3, no exact value could be estimated from the data, but a minimum length of 20 nm is required for appropriate fitting of the data. Correspondingly, chains might fold in this case, as the maximum contour length at a degree of polymerization of 84 is ≈30 nm. The appearance of π-stacked chains for PTHS 3 is further corroborated by a slight increase in radius compared to the smaller polymers. Nevertheless, it is surprising that no larger aggregates are formed, and the features in the absorption spectrum (maximum at 552 nm and strong shoulder at 580 nm), which are characteristic for crystalline polythiophene, appear already with the mostly stretched conformation and very few stacked chains. The extended π-conjugation of the backbone therefore seems to be a decisive factor for the observed optical features of the polymer in solution and larger π–π stacks are not required. Increasing the ionic strength of the solution by adding salt significantly alters the absorbance of this polymer, as the characteristic features disappear in the spectra and a single peak appears at 510 nm. We assume that the coulomb repulsion is shielded and, thus, the polymer adapts a more coiled conformation limiting the conjugation length and potential aggregates are dissolved. More drastic effects are observed in the fluorescence spectra, where after an initial jump a linear correlation between ionic strength and fluorescence intensity was found. The polymer appears quite sensitive to changes in the ionic environment, which is an attractive feature for potential applications as a sensor system. Further studies in this direction are currently being considered. In this regard, the combination with an equivalent cationic CPE was also tested for the resulting optical properties. While to our surprise no aggregation or significant effects became apparent in the absorption spectrum when mixing both CPEs at equimolar ratios, the fluorescence is mostly quenched. Consequently, the oppositely charged polymers must interact, but the rigid conformation of the anionic PTHS seems to be maintained as the characteristic absorption features are still present. Considering the strong fluorescence of the cationic polymer if freely dissolved, these ionic complexes may represent an interesting opportunity to create sensor systems based on competition. Further studies on the presented system are currently being considered, probing the full potential of these interesting coacervates.

Overall, the unique characteristics of the presented regioregular anionic CPEs and the ability to tune their length opens access to unprecedented optical features and unique solution structures. Our observations substantiate the previously mentioned need for well-defined CPEs with regioregular conformation and defined molar masses,[28] as distinct correlations in solution were discovered. However, based on these correlations new opportunities might arise to design more specific and selective sensor materials or create efficient aqueous electrochemical devices.[1,10,70]

4. Experimental Section

All reagents were purchased from commercial suppliers and used without further purification. The monomer 2,5-dibromo-3(6-bromohexyl)thiophene was prepared according to procedures reported in literature.[71,72] The polymers were also synthesized as reported previously.[49] ^{1}H NMR (300 MHz) spectra were recorded on a Bruker AC 300 spectrometer and calibrated relative to the respective solvent resonance signal. SEC measurements were carried out in THF with two Varian MIXED-C columns (300 × 7.5 mm) at room temperature and a flow rate of 0.5 mL min^{-1} using an UV detector (Waters model 486) with 254 nm detector wavelength and a refractive index detector (Waters model 410). Polystyrene was used for calibration in combination with *o*-DCB as an internal standard. MALDI-Tof-MS measurements were performed on a Bruker Reflex III using Dithranol as matrix and a mixture of 1000:1 (Matrix:Polymer). UV–vis spectra were recorded on a Jasco V-670 spectrophotometer. The samples were either prepared in a 10 mm or in a 0.1 mm cuvette for high concentration guaranteeing an optical density between 0.1 and 1. The fluorescence was measured with a Jasco FP-8600 spectrofluorometer in 10 mm optical cuvettes. If not stated otherwise, the samples were excited in the corresponding absorption maxima, and the measurement range was adjusted to keep a minimum

difference to the excitation wavelength of 10 nm. Samples for TEM were prepared by dropping a 1 wt.% solution of the polymer onto a copper grid and soaking up the remaining solution after 1 min of impregnation. The measurements were carried out on a Zeiss EM922 Omega.

SANS was carried out on the Sans2D small-angle diffractometer at the ISIS Pulsed Neutron Source (STFC Rutherford Appleton Laboratory, Didcot, U.K.).[73] A collimation length of 4 m and incident wavelength range of 1.75 – 16.5 Å was employed. Data were measured simultaneously on two 1 m^2 detectors to give a q-range of 0.0045 – 1.00 $Å^{-1}$. The small-angle detector was positioned 4 m from the sample and offset vertically by 60 mm and sideways by 100 mm. The wide-angle detector was positioned 2.4 m from the sample, offset sideways by 980 mm, and rotated to face the sample. q is defined as:

$$q = \frac{4\pi \sin\frac{\theta}{2}}{\lambda} \quad (1)$$

where θ is the scattering angle and λ is the incident neutron wavelength. The beam diameter was 8 mm. Each raw scattering data set was corrected for the detector efficiencies, sample transmission, and background scattering and converted to scattering cross-section data ($\partial\Sigma/\partial\Omega$ vs q) using the instrument-specific software.[74] These data were placed on an absolute scale (cm^{-1}) using the scattering from a standard sample (a solid blend of hydrogenous and perdeuterated polystyrene) in accordance with established procedures.[75]

Supporting Information

Supporting Information is available from the Wiley Online Library or from the author.

Acknowledgements

Financial support from the Bavarian State Ministry for Science and Arts (under SOLTECH project) and the Elitenetzwerk Bayern (ENB), Macromolecular Science, are kindly acknowledged. JCB further thanks the German Science Foundation (DFG) for generous funding within the Emmy-Noether Programme (Project-ID: 358263073). The authors further thank M. Fried and H. Wietasch for their support in the synthesis of the monomers. M. Drechsler is further acknowledged for the TEM analysis.

Open access funding enabled and organized by Projekt DEAL.

Conflict of Interest

The authors declare no conflict of interest.

Data Availability Statement

The data that support the findings of this study are available from the corresponding author upon reasonable request.

Keywords

conjugated polyelectrolytes, kumada catalyst transfer polymerization, neutron scattering, salt concentrations, π-interactions

Received: June 30, 2023
Revised: July 28, 2023
Published online: August 15, 2023

[1] A. Duarte, K.-Y. Pu, B. Liu, G. C. Bazan, *Chem. Mater.* **2010**, *23*, 501.
[2] Y. Liu, V. V. Duzhko, Z. A. Page, T. Emrick, T. P. Russell, *Acc. Chem. Res.* **2016**, *49*, 2478.
[3] Z. He, H. Wu, Y. Cao, *Adv. Mater.* **2014**, *26*, 1006.
[4] C. V. Hoven, A. Garcia, G. C. Bazan, T.-Q. Nguyen, *Adv. Mater.* **2008**, *20*, 3793.
[5] E. W. H. Jager, E. Smela, O. Inganäs, *Science* **2000**, *290*, 1540.
[6] E. Zeglio, M. Vagin, C. Musumeci, F. N. Ajjan, R. Gabrielsson, X. T. Trinh, N. T. Son, A. Maziz, N. Solin, O. Inganäs, *Chem. Mater.* **2015**, *27*, 6385.
[7] K. P. R. Nilsson, O. Inganäs, *Nat. Mater.* **2003**, *2*, 419.
[8] M. Leclerc, *Adv. Mater.* **1999**, *11*, 1491.
[9] K. E. Achyuthan, T. S. Bergstedt, L. Chen, R. M. Jones, S. Kumaraswamy, S. A. Kushon, K. D. Ley, L. Lu, D. Mcbranch, H. Mukundan, F. Rininsland, X. Shi, W. Xia, D. G. Whitten, *J. Mater. Chem.* **2005**, *15*, 2648.
[10] C. Zhu, L. Liu, Q. Yang, F. Lv, S. Wang, *Chem. Rev.* **2012**, *112*, 4687.
[11] K. Li, B. Liu, *Polym. Chem.* **2010**, *1*, 252.
[12] J. Han, H. Cheng, B. Wang, M. S. Braun, X. Fan, M. Bender, W. Huang, C. Domhan, W. Mier, T. Lindner, K. Seehafer, M. Wink, U. H. F. Bunz, *Angew. Chem., Int. Ed.* **2017**, *56*, 15246.
[13] H. Sun, K. S. Schanze, *ACS Appl. Mater. Interfaces* **2022**, *14*, 20506.
[14] T. I. Wallow, B. M. Novak, *J. Am. Chem. Soc.* **1991**, *113*, 7411.
[15] I. U. Rau, M. Rehahn, *Polymer* **1993**, *34*, 2889.
[16] R. Rulkens, M. Schulze, G. Wegner, *Macromol. Rapid Commun.* **1994**, *15*, 669.
[17] G. Brodowski, A. Horvath, M. Ballauff, M. Rehahn, *Macromolecules* **1996**, *29*, 6962.
[18] S. Kim, J. Jackiw, E. Robinson, K. S. Schanze, J. R. Reynolds, J. Baur, M. F. Rubner, D. Boils, D. Boils, *Macromolecules* **1998**, *31*, 964.
[19] C. Tan, M. R. Pinto, K. S. Schanze, *Chem. Commun.* **2002**, 446.
[20] C. Tan, E. Atas, J. G. Müller, M. R. Pinto, V. D. Kleiman, K. S. Schanze, *J. Am. Chem. Soc.* **2004**, *126*, 13685.
[21] X. Zhao, M. R. Pinto, L. M. Hardison, J. Mwaura, J. Müller, H. Jiang, D. Witker, V. D. Kleiman, J. R. Reynolds, K. S. Schanze, *Macromolecules* **2006**, *39*, 6355.
[22] S. W. Thomas, G. D. Joly, T. M. Swager, *Chem. Rev.* **2007**, *107*, 1339.
[23] Y. Liu, K. Ogawa, K. S. Schanze, *J. Photochem. Photobiol., C* **2009**, *10*, 173.
[24] B. Liu, W.-L. Yu, Y.-H. Lai, W. Huang, *Macromolecules* **2002**, *35*, 4975.
[25] F. Huang, H. Wu, D. Wang, W. Yang, Y. Cao, *Chem. Mater.* **2004**, *16*, 708.
[26] H. D. Burrows, V. M. M. Lobo, J. Pina, M. L. Ramos, J. Seixas De Melo, A. J. M. Valente, M. J. Tapia, S. Pradhan, U. Scherf, *Macromolecules* **2004**, *37*, 7425.
[27] A. O. Patil, Y. Ikenoue, F. Wudl, A. J. Heeger, *J. Am. Chem. Soc.* **1987**, *109*, 1858.
[28] G. Sinsinbar, A. Palaniappan, U. H. Yildiz, B. Liedberg, *ACS Sens.* **2022**, *7*, 686.
[29] B. Mcculloch, V. Ho, M. Hoarfrost, C. Stanley, C. Do, W. T. Heller, R. A. Segalman, *Macromolecules* **2013**, *46*, 1899.
[30] H.-A. Ho, A. Najari, M. Leclerc, *Acc. Chem. Res.* **2008**, *41*, 168.
[31] B. Liu, G. C. Bazan, *Chem. Mater.* **2004**, *16*, 4467.
[32] H. Bai, H. Lu, X. Fu, E. Zhang, F. Lv, L. Liu, S. Wang, *Biomacromolecules* **2018**, *19*, 2117.
[33] P. C. Ewbank, R. S. Loewe, L. Zhai, J. Reddinger, G. Sauvé, R. D. Mccullough, *Tetrahedron* **2004**, *60*, 11269.
[34] R. D. Mccullough, P. C. Ewbank, R. S. Loewe, *J. Am. Chem. Soc.* **1997**, *119*, 633.
[35] Z. Yao, Y. Yang, X. Chen, X. Hu, L. Zhang, L. Liu, Y. Zhao, H.-C. Wu, *Anal. Chem.* **2013**, *85*, 5650.

[36] A. Åslund, A. Herland, P. Hammarström, K. P. R. Nilsson, B.-H. Jonsson, O. Inganäs, P. Konradsson, *Bioconjugate Chem.* **2007**, *18*, 1860.
[37] K. P. R. Nilsson, P. Hammarström, F. Ahlgren, A. Herland, E. A. Schnell, M. Lindgren, G. T. Westermark, O. Inganäs, *ChemBioChem* **2006**, *7*, 1096.
[38] K. P. R. Nilsson, A. Herland, P. Hammarström, O. Inganäs, *Biochemistry* **2005**, *44*, 3718.
[39] G. Sinsinbar, S. Gudlur, S. E. Wood, G. Ammanath, H. U. Yildiz, P. Alagappan, M. Mrksich, B. Liedberg, *Angew. Chem., Int. Ed.* **2020**, *59*, 18068.
[40] Z. Yao, X. Hu, B. Huang, L. Zhang, L. Liu, Y. Zhao, H.-C. Wu, *ACS Appl. Mater. Interfaces* **2013**, *5*, 5783.
[41] Z. Yao, X. Hu, W. Ma, X. Chen, L. Zhang, J. Yu, Y. Zhao, H.-C. Wu, *Analyst* **2013**, *138*, 5572.
[42] M. Kraft, S. Adamczyk, A. Polywka, K. Zilberberg, C. Weijtens, J. Meyer, P. Görrn, T. Riedl, U. Scherf, *ACS Appl. Mater. Interfaces* **2014**, *6*, 11758.
[43] J. E. Houston, M. Kraft, I. Mooney, A. E. Terry, U. Scherf, R. C. Evans, *Langmuir* **2016**, *32*, 8141.
[44] J. E. Houston, M. Kraft, U. Scherf, R. C. Evans, *Phys. Chem. Chem. Phys.* **2016**, *18*, 12423.
[45] M. Knaapila, R. C. Evans, V. M. Garamus, L. Almásy, N. K. Székely, A. Gutacker, U. Scherf, H. D. Burrows, *Langmuir* **2010**, *26*, 15634.
[46] M. Knaapila, R. C. Evans, A. Gutacker, V. M. Garamus, N. K. Székely, U. Scherf, H. D. Burrows, *Soft Matter* **2011**, *7*, 6863.
[47] A. Gutacker, S. Adamczyk, A. Helfer, L. E. Garner, R. C. Evans, S. M. Fonseca, M. Knaapila, G. C. Bazan, H. D. Burrows, U. Scherf, *J. Mater. Chem.* **2010**, *20*, 1423.
[48] R. D. Mccullough, P. C. Ewbank, *Synth. Met.* **1997**, *84*, 311.
[49] J. C. Brendel, M. M. Schmidt, G. Hagen, R. Moos, M. Thelakkat, *Chem. Mater.* **2014**, *26*, 1992.
[50] S. Inal, J. Rivnay, P. Leleux, M. Ferro, M. Ramuz, J. C. Brendel, M. M. Schmidt, M. Thelakkat, G. G. Malliaras, *Adv. Mater.* **2014**, *26*, 7450.
[51] P. Schmode, D. Ohayon, P. M. Reichstein, A. Savva, S. Inal, M. Thelakkat, *Chem. Mater.* **2019**, *31*, 5286.
[52] M. M. Schmidt, M. Elmahmoudy, G. G. Malliaras, S. Inal, M. Thelakkat, *Macromol. Chem. Phys.* **2018**, *219*, 1700374.
[53] A. Kiriy, V. Senkovskyy, M. Sommer, *Macromol. Rapid Commun.* **2011**, *32*, 1503.
[54] R. H. Lohwasser, M. Thelakkat, *Macromolecules* **2011**, *44*, 3388.
[55] C. Scharsich, R. H. Lohwasser, M. Sommer, U. Asawapirom, U. Scherf, M. Thelakkat, D. Neher, A. Köhler, *J. Polym. Sci., B: Polym. Phys.* **2012**, *50*, 442.
[56] F. C. Spano, *J. Chem. Phys.* **2005**, *122*, 234701.
[57] H. Meier, U. Stalmach, H. Kolshorn, *Acta Polym.* **1997**, *48*, 379.
[58] M. Chayer, K. Faïd, M. Leclerc, *Chem. Mater.* **1997**, *9*, 2902.
[59] A. Garcia, T.-Q. Nguyen, *J. Phys. Chem. C* **2008**, *112*, 7054.
[60] M. Brinkmann, P. Rannou, *Adv. Funct. Mater.* **2007**, *17*, 101.
[61] I. Breßler, J. Kohlbrecher, A. F. Thünemann, *J. Appl. Crystallogr.* **2015**, *48*, 1587.
[62] J. B. Hayter, J. Penfold, *Mol. Phys.* **1981**, *42*, 109.
[63] A. Dobrynin, M. Rubinstein, *Prog. Polym. Sci.* **2005**, *30*, 1049.
[64] S. Förster, M. Schmidt, *Adv. Polym. Sci.* **1995**, *120*, 51.
[65] S. Förster, M. Schmidt, M. Antonietti, *Polymer* **1990**, *31*, 781.
[66] T. Hofmann, R. G. Winkler, P. Reineker, *J. Chem. Phys.* **2003**, *119*, 2406.
[67] S. P. O. Danielsen, T.-Q. Nguyen, G. H. Fredrickson, R. A. Segalman, *ACS Macro Lett.* **2019**, *8*, 88.
[68] A. R. Johnston, S. L. Perry, A. L. Ayzner, *Chem. Mater.* **2021**, *33*, 1116.
[69] B. Yu, A. M. Rumyantsev, N. E. Jackson, H. Liang, J. M. Ting, S. Meng, M. V. Tirrell, J. J. de Pablo, *Mol. Syst. Des. Eng.* **2021**, *6*, 790.
[70] S. Inal, J. Rivnay, A.-O. Suiu, G. G. Malliaras, I. Mcculloch, *Acc. Chem. Res.* **2018**, *51*, 1368.
[71] P. Bäuerle, F. Würthner, S. Heid, *Angew. Chem.* **1990**, *102*, 414.
[72] S. Miyanishi, K. Tajima, K. Hashimoto, *Macromolecules* **2009**, *42*, 1610.
[73] R. K. Heenan, S. E. Rogers, D. Turner, A. E. Terry, J. Treadgold, S. M. King, *J. Neutron Res.* **2011**, *22*, 19.
[74] http://www.mantidproject.org, **2015**.
[75] G. D. Wignall, F. S. Bates, *J. Appl. Crystallogr.* **1987**, *20*, 28.

